Highlights of Spanish Astrophysics XII, Proceedings of the XVI Scientific Meeting of the Spanish Astronomical Society held on July 15 - 19, 2024, in Granada, Spain. M. Manteiga, F. González Galindo, A. Labiano Ortega, M. Martínez González, N. Rea, M. Romero Gómez, A. Ulla Miguel, G. Yepes, C. Rodríguez López, A. Gómez García and C. Dafonte (eds.), 2025

MIri Characterization Of Nearby Infrared galaxy Centers (MICONIC): first results of the JWST MIRI/MRS GTO program

Hermosa Muñoz, L.[1], **Alonso-Herrero, A.**[1], **on behalf of the MICONIC team**

[1] Centro de Astrobiología (CAB) CSIC-INTA, Camino Bajo del Castillo s/n, 28692 Villanueva de la Cañada, Madrid, Spain

Abstract

The bright mid-infrared (mid-IR) emission of local luminous and ultraluminous infrared galaxies (LIRGs and ULIRGs) is due to the presence of an active galactic nucleus (AGN) and/or intense star formation processes. These galaxies are mostly interacting/merger systems with a complex interplay between large amounts of gas and dust capable of triggering outflows and/or inflows. The James Webb Space Telescope (JWST) offers a new opportunity to study the properties of (U)LIRGs with an unprecedented combination of high spatial and spectral resolution in the mid-IR. We present the first results from the guaranteed time observations (GTO) program termed MIri Characterization Of Nearby Infrared galaxy Centers (MICONIC). This program obtained spatially resolved 5-28micron observations of several local galaxies using the MIRI Spectrograph (MRS). Particularly, we will discuss the MRS-derived properties of the ionised and molecular gas outflows of two well-known nearby (U)LIRGs, namely Mrk 231 and NGC 6240.

1 Introduction

We present the guaranteed time observations (GTO) program termed *Mid-Infrared Characterization Of Nearby Iconic galaxy Centers* (MICONIC) of the Mid-Infrared Instrument (MIRI) [32, 40, 41] European Consortium. This program aims to study nearby (ultra)luminous infrared galaxies (U/LIRGs) such as Mrk 231 [4], Arp 220, NGC 6240 [22], as well as the radio galaxy Centaurus A, the low metallicity galaxy SBS 0335-052, and the region surrounding SgrA* in our Galaxy. These targets have been selected in collaboration with the GTO program for nearby galaxies of the NIRSpec team [31, 36], providing a complete near- and mid-infrared (near- and mid-IR) view into the nuclei and circumnuclear regions of these galaxies. Within MICONIC, all the objects were observed using the medium-resolution spectrometer

(MRS) of the MIRI instrument on board of the James Webb Space Telescope (JWST) [20]. This instrument covers a total wavelength range from 4.9 to 27.9 μm through four different integral field units (IFUs), referred to as channels. These channels have different field-of-views (FoV, from 3.2" $\times$ 3.7" in channel 1 up to 6.6" $\times$ 7.7" in channel 4), spatial (0.13" to 0.35"), and spectral ($\sim$3700 to $\sim$1500) resolutions [25, 6]. With the unprecedented resolution obtained with JWST data, our aim is to carry out a spatially resolved study of the mid-IR emission of the aforementioned targets, providing a comprehensive view of their properties. In particular, we can simultaneously analyse the ionised, warm molecular, and recombination emission lines, molecular absorption features, and polycyclic aromatic hydrocarbon (PAH) features. This allows us to evaluate the star formation (SF), the extinction, temperature, density, and ionisation source of the gas, potential outflows in the different gas phases, and assess the presence of an active galactic nucleus (AGN) in these systems, among other aspects. Here we focus on the results obtained for Mrk 231 [4] and NGC 6240 [22].

NGC 6240 is a LIRG ($\log(L_{IR}/L_{\odot}) = 11.93$ [23]) and a galaxy merger located at 111 Mpc. It hosts two supermassive black holes detected in X-rays [34], separated by $\sim$ 1.5" = 740 pc [24]. Both of them are classified as AGN, with the northern nucleus (N) being a low ionisation nuclear emission-line region (LINER) and the southern nucleus (S) a type-2 Seyfert, based on optical line ratios [29]. The gas in this system has a complex morphology and dynamics, with the ionised gas extending up to $\sim$ 90 kpc [37, 42]. Several massive outflows have been detected through different gas phases, driven by both the AGN and the intense SF [12, 29, 15].

Mrk 231 is a ULIRG ($\log(L_{IR}/L_{\odot}) = 12.60$), and the nearest broad absorption line (BAL) quasar [26, 33], located at a distance of 188 Mpc (1" = 837 pc, [17]). This source is known to have a strong infrared continuum [8], that could only be explained by the presence of both an AGN and a powerful nuclear starburst ([28] and references therein). Several wide-angle outflows have been detected in all gas phases, with velocities from a few hundreds up to more than 1000 km s^{-1} in some phases, driven by either the quasar, strong SF activity, and/or the radio jet [18, 11, 16, 17, 39].

2 Results and discussion

2.1 NGC 6240

This system has already been studied in the mid-IR with long-slit Spitzer/IRS and ground-based spectroscopy [7, 1]. Several ionised and molecular gas lines have been detected, as well as strong PAH emission, specially around the S nucleus [1]. Focusing on the ionised emission lines, the Spitzer detection at 4" resolution of high-excitation lines (ionisation potential, IP > 90 eV), such as [Ne V] at 14.32μm, was attributed to the presence of a buried AGN, whereas low-excitation lines, such as [Ne II] at 12.81μm and [Ne III] at 15.55μm, were associated to the central starburst [7].

With the MRS/MIRI data we resolved for the first time the two nuclei in the 5-28μm spectral range, with a total of 32 different emission lines detected (20 ionised gas with IPs ranging from 7.6 to 126 eV, 10 warm molecular H_2, and two hydrogen recombination lines). The lines for both nuclei show very complex, broad profiles, highly non-symmetrical for the

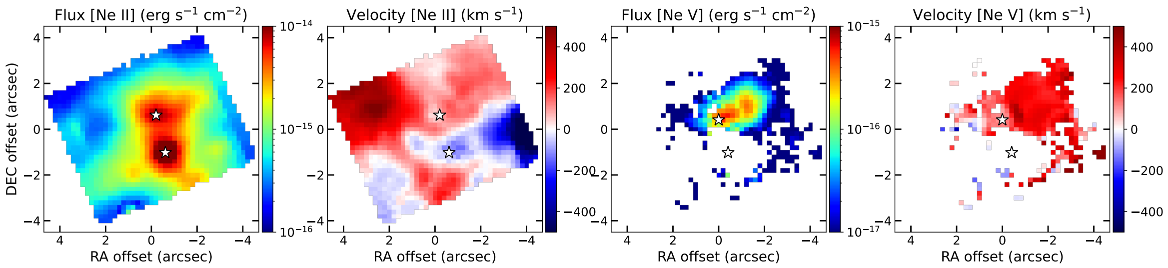

Figure 1: Spatially resolved maps (flux and velocity) obtained with a single Gaussian modelling of the low ([Ne II]) and high ([Ne V]) excitation lines in NGC 6240. The position of the nuclei are indicated with white stars. The total FoV is 9.4" ×9.0" (i.e. 4.9 kpc×4.7 kpc).

S nucleus. In particular, for the N nucleus the average full-width at half maximum (FWHM) of the lines is $\sim 700\,\mathrm{km\,s^{-1}}$, whereas it reaches up to $\sim$1500 $\mathrm{km\,s^{-1}}$ for the S nucleus. One important difference between the spectra of both nuclei is that the high excitation lines (IP > 90 eV) are detected in the N nucleus, but are faint for the S nucleus.

We created spatially-resolved maps of all the ionised gas emission lines and found notable differences between low and high excitation lines (see Fig. 1). The former lines (such as [Ne II] and [Ar II] at 6.98μm) are detected over the whole FoV, with the peak of the emission in both nuclei and several clumps, whereas the high excitation lines (such as [Ne V] and [Ne VI] at 7.46μm) are only detected in the N nucleus, extending in a bubble-like structure north-west from the N nucleus, up to $\sim$ 2" (i.e. $\sim$1 kpc). On the one hand, the kinematics of the low excitation lines is perturbed and uncorrelated with the stellar discs [29], showing non-rotational motions and a "v"-like shaped velocity dispersion (σ), with values reaching more than 500 $\mathrm{km\,s^{-1}}$. On the other hand, the high excitation lines show completely redshifted velocities and low σ ($\sim 200\,\mathrm{km\,s^{-1}}$). Its morphology suggests the presence of an ionised gas outflow (see full discussion in [22]), coincident with the direction of the optical Hα bubble detected by [29].

Given that some of the high excitation lines fall within PAH features, that are really strong in this source (e.g. [Ne VI] at 7.46μm with the PAH at 7.7μm), they could be either absent, or simply "buried" in the spectra. To understand this, we used the tool presented in [14] to model the continuum and PAH features of the integrated spectra (r$\sim$ 0.7") for both nuclei. After the modelling, for the S nucleus both [Ne VI] and [Mg V] lines were detected in the integrated spectrum. This indicates that both the strong PAH features and the mid-IR continuum in the S nucleus were "burying" the high excitation lines, which proves the AGN nature of both nuclei.

2.2 Mrk 231

As for NGC 6240, this system has already been studied with ground and Spitzer mid-IR spectroscopy [21, 8, 38, 2, 3]. The spectrum showed a strong mid-IR continuum with only a few low excitation, and H_2 emission lines, and no high excitation lines. Several works of this source with imaging, spectroscopy and polarimetry proved that the AGN is the main contributor to the total mid-IR continuum emission of this galaxy [2, 3, 28].

With the MIRI/MRS data, the nuclear spectrum shows a strong and steeply rising mid-IR continuum (see Fig. 2 in [4]), mostly dominated by the bright point source. We detected few low ionisation ionised gas (up to 41 eV) with relatively narrow profiles (FWHM$\sim$280 km s^{-1}), in contrast to other U/LIRGs observed with JWST (see Sect. 2.1, [30, 19, 5]). Some of the lines (e.g. [Ar II] and [Ar III] at 8.99μm), undetected with Spitzer, are seen in the (circum)nuclear region. Similarly to previous studies [8], high excitation lines (i.e. [Ne VI] and [Mg V]) were not detected in the spectra. These also would be located near absorption features, that could affect their detection. We simulated the expected flux for these lines based on the X-ray luminosity of Mrk 231, and the detection of these lines in two local LIRGs (NGC 6240-N, see Sect. 2.1 and [22], and NGC 7469 [9]). We determined that the high excitation lines remain undetected if Mrk 231 is an intrinsically weak quasar in X-rays (see also [35]), summed up to the strong mid-IR continuum of the source, and the presence of continuum structure due to absorption features [4].

Additionally, we detected warm molecular lines H_2 (0-0) from S(8) to S(1), relatively weak PAH features (at 6.2, 11.3, 12.7 and 16.5 μm), and multiple absorption features appearing in both gas and ice phases (e.g. H_2O) in the integrated spectrum. The PAH low equivalent widths reflect the influence of the AGN, that produces a strong mid-IR continuum. However, both the PAHs and the low excitation lines are detected throughout all the MRS's FoV, which is an indication of SF activity. In fact, several SF regions, that were already known from previous observations [27], are traced with the [Ne II] emission (see Fig. 2). Although the emission lines are contaminated by the strong unresolved AGN source, after subtracting the point-spread function, resolved emission was detected for [Ne II] and [Ar II] with an estimated size $\sim$ 420 pc. Thus, these lines are tracing the presence of a nuclear starburst, with a size consistent to previous optical, near-IR, and radio observations [27, 13, 10].

The low excitation line nuclear profiles show faint blue wings, with the largest velocities found for the [Ne II] line (maximum $\sim$ 540 km s^{-1}). We attributed these features to the presence of a starburst-driven outflow, which is likely perpendicular to the nearly face-on disc (see Fig. 15 in [4]), although we cannot rule out some AGN contribution. We also detected non-rotational motions for the warm molecular gas (see Fig. 2), but with mild velocities with respect to those seen for other tracers [17]. The system is known to have some expanding shells and super-bubbles associated to the intense SF [26]. We detected several SF regions associated with some of the shells, as well as blueshifted velocities (few km s^{-1}) and enhanced velocity dispersions for the H_2 gas, which appear to be related to the expanding shells.

3 Conclusions

We have performed for the first time spatially-resolved, detailed studies in the 5-28 μm spectral range for both Mrk 231 and NGC 6240. Both systems are complex, with the presence of non-rotational motions, a strong mid-IR continuum, and intense SF and AGN activity. The new JWST/MIRI data have allowed us to understand with unprecedented resolution the

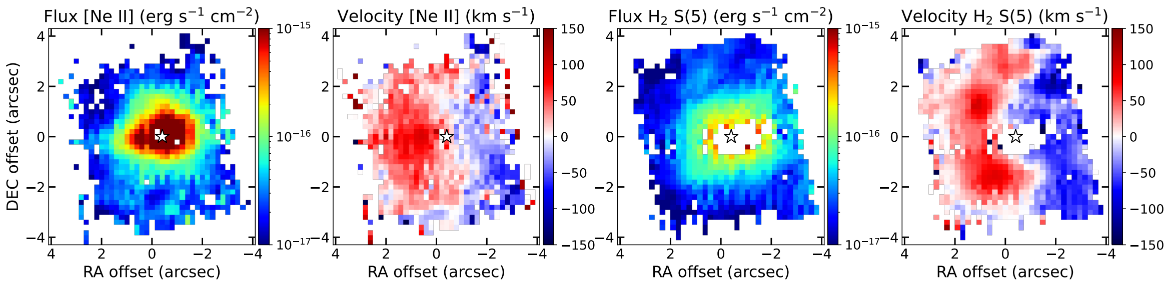

Figure 2: Spatially resolved maps (flux and velocity) obtained with a single Gaussian modelling of the low excitation ([Ne II]) and warm molecular gas (H_2 (0-0) S5) lines in Mrk 231. The photometric centre is indicated with a white star. The total FoV is 8.2"×8.6" (i.e. 6.8 kpc×7.2 kpc).

(circum)nuclear properties of these well-known local U/LIRGs. The detailed discussion on these data for Mrk 231 and NGC 6240 are presented in [4] and [22], respectively.

Acknowledgements

LHM and AAH thank the members of MICONIC for their invaluable contributions and support throughout the course of these works. We acknowledge financial support by the grant PID2021-124665NB-I00 funded by the Spanish Ministry of Science and Innovation and the State Agency of Research MCIN/AEI/10.13039/501100011033 PID2021-124665NB-I00 and ERDF A way of making Europe. This work is based on observations made with the NASA/ESA/CSA James Webb Space Telescope. The data were obtained from the Mikulski Archive for Space Telescopes at the Space Telescope Science Institute, which is operated by the Association of Universities for Research in Astronomy, Inc., under NASA contract NAS5-03127 for JWST; and from the European JWST archive (eJWST) operated by the ESDC. These observations are associated with programs 1265 and 1268.

References

[1] Alonso-Herrero, A., Ramos Almeida, C., Esquej, P., et al. 2014, MNRAS, 443, 2766

[2] Alonso-Herrero, A., Esquej, P., Roche, P. F., et al. 2016a, MNRAS, 455, 563

[3] Alonso-Herrero, A., Poulton, R., Roche, P. F., et al. 2016b, MNRAS, 463, 2405

[4] Alonso-Herrero, A., Hermosa Muñoz, L., Labiano, A., et al. 2024, A&A, 690, A95

[5] Álvarez-Márquez, J., Labiano, A., Guillard, P., et al. 2023, A&A, 672, A108

[6] Argyriou, I., Glasse, A., Law, D. R., et al. 2023, A&A, 675, A111

[7] Armus, L., Bernard-Salas, J., Spoon, H. W. W., et al. 2006, ApJ, 640, 204

[8] Armus, L., Charmandaris, V., Bernard-Salas, J., et al. 2007, ApJ, 656, 148

[9] Armus, L., Lai, T., U, V., et al. 2023, ApJ, 942, L37

[10] Carilli, C. L., Wrobel, J. M. & Ulvestad, J. S. 1998, AJ, 115, 928

[11] Cicone, C., Feruglio, C., Maiolino, R., et al. 2012, A&A, 543, A99

[12] Cicone, C., Severgnini, P., Papadopoulos, P. P., et al. 2018, ApJ, 863, 143

[13] Davies, R. I., Tacconi, L. J., & Genzel, R. 2004, ApJ, 613, 781

[14] Donnan, F. R., Garcıía-Bernete, I., Rigopoulou, D., et al. 2024, MNRAS, 529, 1386

[15] Fabbiano, G., Paggi, A., Karovska, M., et al. 2020, ApJ, 902, 49

[16] Feruglio, C., Maiolino, R., Piconcelli, E., et al. 2010, A&A, 518, L155

[17] Feruglio, C., Fiore, F., Carniani, S., et al. 2015, A&A, 583, A99 1148

[18] Fischer, J., Sturm, E., González-Alfonso, E., et al. 2010, A&A, 518, L41

[19] García-Bernete, I., Rigopoulou, D., Alonso-Herrero, A., et al. 2022b, A&A, 666, 1157 L5

[20] Gardner, J. P., Mather, J. C., Abbott, R., et al. 2023, PASP, 135, 068001

[21] Genzel, R., Lutz, D., Sturm, E., et al. 1998, ApJ, 498, 579

[22] Hermosa Muñoz, L., Alonso-Herrero, A., Labiano, A., et al. 2024, arXiv e-prints: 2412.14707

[23] Kim, D. C., Evans, A. S., Vavilkin, T., et al. 2013, ApJ, 768, 102

[24] Komossa, S., Burwitz, V., Hasinger, G., et al. 2003, ApJ, 582, L15

[25] Labiano, A., Argyriou, I., Álvarez-Márquez, J., et al. 2021, A&A, 656, A57

[26] Lipari, S., Terlevich, R., Zheng, W., et al. 2005, MNRAS, 360, 416

[27] Lipari, S., Sanchez, S. F., Bergmann, M., et al. 2009, MNRAS, 392, 1295

[28] López-Rodríguez, E., Packham, C., et al. 2017, MNRAS, 464, 1762

[29] Müller-Sánchez, F., Nevin, R., Comerford, J. M., et al. 2018, Nature, 556, 345

[30] Pereira-Santaella, M., Álvarez-Márquez, J., García-Bernete, I., et al. 2022, A&A, 665, L11

[31] Perna, M., Arribas, S., Lamperti, I., et al. 2024, A&A, 690, A171

[32] Rieke, G. H., Wright, G. S., Böker, T., et al. 2015, PASP, 127, 584

[33] Rupke, D. S., Veilleux, S., & Sanders, D. B. 2005, ApJ, 632, 751

[34] Scoville, N., Sheth, K., Walter, F., et al. 2015, ApJ, 800, 70

[35] Teng, S. H., Brandt, W. N., Harrison, F. A., et al. 2014, ApJ, 785, 19

[36] Ulivi, L., Perna, M., Lamperti, I., et al. 2025, A&A, 693, A36

[37] Veilleux, S., Shopbell, P. L., Rupke, D. S., et al. 2003, AJ, 126, 2185

[38] Veilleux, S., Rupke, D. S. N., Kim, D. C., et al. 2009, ApJS, 182, 628

[39] Veilleux, S., Meléndez, M., Tripp, et al. 2016, ApJ, 825, 42

[40] Wright, G. S., Wright, D., Goodson, G. B., et al. 2015, PASP, 127, 595

[41] Wright, G. S., Rieke, G. H., Glasse, A., et al. 2023, PASP, 135, 048003

[42] Yoshida, M., Yagi, M., Ohyama, Y., et al. 2016, ApJ, 820, 48